

Prediction of clear-water scour around submarine pipeline under steady flow condition

Zhiyong Zhang^{1,2}, Bing Shi², Yakun Guo³, Daoyi Chen⁴

1. Zhejiang Institute of Hydraulics and Estuary, Hangzhou, 310020, China.

zhangzy@zjwater.gov.cn

2. College of Engineering, Ocean University of China, Qingdao, 266100, China.

sediment@ouc.edu.cn

3. School of Engineering, University of Bradford, Bradford, BD7 1DP, Corresponding author,

Email: y.guo16@bradford.ac.uk

4. Division of Ocean Science and Technology, Graduate School at Shenzhen, Tsinghua

University, China. chen.daoyi@sz.tsinghua.edu.cn

Abstract: Local scour around submarine pipelines can affect the stability of the pipeline. The accurate estimation of the scour around submarine pipelines has been a hot topic of research among marine engineers. This paper presents results from a numerical study of clear-water scour depth below a submarine pipeline for a range of the steady flow conditions. The flow field around the pipeline under scour equilibrium condition is numerically simulated by solving the Reynolds-Averaged Navier-Stokes (RANS) equations with the standard $k-\varepsilon$ turbulence closure. The flow discharge through the scour hole for various flow conditions is investigated. The results are used to establish the relationship between the flow discharge and the maximum scour depth. Incorporated with the Colebrook-White equation, the bed shear stress is obtained and an iterative method is proposed to predict the scour depth around the submarine pipeline. The calculated scour depths using the present method agree well with the

laboratory measurements, with the average absolute relative error being smaller than that using previous methods, indicating that the proposed method can be used to predict the clear-water scour around the submarine pipeline with satisfactory accuracy.

Key Words: submarine pipeline; steady flow; scour depth; scour hole discharge

Notation:

ARER-absolute relative error of prediction	scour depth
D -pipeline diameter	s -the ratio of sediment density over water
d_s -maximum scour depth	density
d_c -scour depth at $x=0$	S_{ij} -mean strain rate tensor
d_{50} -median sediment size	t -time
G_k -the generation of k induced by the mean velocity gradients	u_i -fluid velocity component, $i=1,2$.
k -turbulent kinetic energy	u_0 -average inflow velocity
k_s -surface roughness height	u_m -flow velocity at surface
m -power law velocity index	u_i' - fluctuation of flow velocity in i direction
p -pressure	V - average flow velocity in the scour hole
q_0 -inflow discharge per unit width below the top of the pipeline	x -horizontal coordinate
q_g -scour hole discharge per unit width	y -vertical coordinate
$(Re)_s$ - the Reynolds number based on the	y_0 -water depth
	y_b -vertical bed position
	ε -turbulent dissipation rate

λ -friction coefficient	θ_{cr} -critical Shields number
μ -the fluid dynamic viscosity	ρ -fluid density
μ_t -the turbulent eddy viscosity	ρ_s - sediment density
ν - fluid kinetic viscosity	τ_b -bed shear stress
ν_T -turbulent viscosity	τ_{cr} -critical bed shear stress
θ -the Shields number	

1 Introduction

Submarine pipelines are usually used to transport oil and gas from offshore to onshore. The installation of pipelines at the seabed will inevitably change the marine hydrodynamic environment, which usually enhances the sediment transport around the pipelines. This in turn causes scour around the pipeline, leading to the suspension of the pipeline. When the length of the suspended pipeline is over a critical value, vortex induced vibration (VIV) occurs which may cause the fatigue failure of the pipeline. Previous study shows that the scour profile/length is usually related to the scour depth (Yang et al. 2012). This means that the scour profile/length around a submarine pipeline can be estimated if the scour depth is known.

Due to the practical engineering importance and applications of submarine pipelines, many studies have been conducted in the past decades to investigate the scour depth under the pipelines. Chao and Hennessy (1972) established a semi-theoretical model to predict the clear-water scour depth based on potential theory. They assumed that the maximum scour depth was reached when the flow induced bed shear stress was equal to the critical bed shear stress for the incipient motion of sediment. Using the scour hole discharge estimated by

potential theory and the wall shear stress calculated by the Colebrook-White equation, they proposed a method (the C-H method) to predict the scour depth. However, as the flow discharge is overestimated, the calculated scour depth is always larger than the practical scour depth. Kjeldsen *et al.* (1973) experimentally studied the relationship between the scour depth and the pipeline diameter as well as the flow velocity. They proposed an empirical equation to estimate the scour depth. However, they did not consider the effect of water depth and sediment size on scour. Ibrahim and Nalluri (1986) investigated the effect of the water depth, the pipeline size and the flow velocity on the scour depth. Jensen *et al.* (1990) conducted laboratory experiments to investigate the scour process. The flow velocity field over the scoured bed was measured and discussed when the equilibrium scour state was reached. Chiew (1991) developed an iterative method (Chiew method) to predict the scour depth underneath the pipeline based on the C-H method. In his study, the curves of scour hole discharge, which had a relationship with the relative water depth, based on the experiment results were used to replace the potential theory. As such, the predicted scour depth was more accurate than that estimated by the C-H method. However, the effect of the scour depth on scour hole discharge was not considered. Moncada-M and Aguirre-Pe (1999) proposed two equations, which were based on the Froude number, to calculate the scour depth and width respectively. Recently, Yang *et al.* (2012) proposed a power law formula to describe the velocity distribution in the scour hole. They used this formula to calculate the wall shear stress based on the open channel hydraulics theory. However, the velocity distribution in the scour hole is more complicated due to the different roughnesses of the seabed and pipelines, thus, the power law may not be applicable in the scour hole.

With the development of computational technology, numerical methods have been applied to simulate the scouring process below the submarine pipeline. Brors (1999) applied the Taylor-Galerkin Finite Element Method (FEM) to solve the two dimensional RANS equations, while sediment transport was calculated using the Finite Difference Method (FDM). The simulated scour evolution was in agreement with the experimental results. However, as indicated by Brors (1999), the considerable computational time was an issue. Liang *et al.* (2004, 2005) applied the sub-grid-scale (SGS) model and $k-\varepsilon$ model to simulate the scour evolution. . In their simulation, the dynamic mesh technology was applied to capture the bed scour evolution. Different time steps for the flow field calculation and sediment transport calculation were applied to improve the computational efficiency. Their simulation results agreed satisfactorily with the experimental measurements. The scour evolution process was also simulated by Zhao and Fernando (2007) who employed the Euler-Euler multiphase model. However, the computational time was very high. Though these studies demonstrate some features of the scour process below the pipelines, the scour equilibrium process received much less research. In particular, the application of the numerical methods to simulate the two or three-dimensional scour equilibrium process is still limited. This is partially due to the considerable computational resources required.

In practical engineering, the semi-theoretical C-H method is often used for its simplicity, to quickly assess the scour state, while the numerical methods are rarely used, mainly due to the high requirement for computing resources. However as aforementioned, the C-H method often overestimates the scour depth due to the overestimation of the flow discharge based on inviscid fluid potential theory. This provides the motivation for this study, which aims to

propose a more accurate and efficient prediction method to estimate the scour around the submarine pipelines. It is expected that such accurate and efficient estimation of the scour characteristics around the submarine pipeline may help offshore engineers to assess the stability of the submarine pipeline due to the potential scour around it, thus propose better protective and preventive measures. In this study, owing to the fact that the non-dimensional equilibrium scour profile has a self- similar form, the scour beds at the various maximum scour depths can be established. The flow field around the submarine pipeline is simulated by solving the Reynolds-Averaged Navier-Stokes (RANS) equations and the standard $k-\varepsilon$ turbulence model. The velocity distributions in the scour hole and the scour hole discharge are then obtained. An empirical formula, which relates the relative scour hole discharge to relative scour depth, is proposed. Incorporating this formula with the Colebrook-White equation, the flow induced bed shear stress can be calculated. The maximum scour depth is then obtained by continuously increasing the scour depth until the calculated bed shear stress is equal to the critical bed shear stress for incipient motion of the bed sediment.

2 Prediction Method

The present prediction method is developed based on the C-H method and Chiew's method. The key point of the present method is to accurately predict the scour hole discharge, taking into consideration the effect of scour depth.

The C-H method calculates the scour hole discharge q_g based on the potential flow theory:

$$\frac{q_g}{q_0} = \frac{\int_{-d_s}^0 u dy}{q_0} = \frac{[d_s + 0.5D - \frac{D^2}{4(2d_s + 0.5D)}]}{D} \quad (1)$$

where d_s is the maximum scour depth; D is the diameter of the pipeline; u is the flow velocity and q_0 refers to the inflow discharge per unit width below the top of the pipeline, which can be calculated as

$$q_0 = \int_0^D u(y) dy = \int_0^D u_m \left(\frac{y}{y_0}\right)^m dy = u_0 D \left(\frac{D}{y_0}\right)^m \quad (2)$$

where m is the power law velocity index; y_0 is the water depth; u_m is the flow velocity at the water surface.

Chiew (1991) proposed a curve based on experimental results to interpolate the scour hole discharge. To facilitate the calculation of the scour hole discharge, Dey and Singh (2007) fitted Chiew's curve using the following equation:

$$\frac{q_g}{q_0} = 0.78 \frac{y_0}{D} (m+0)^2 \quad (3)$$

It can be seen that Eq. (3) only considers the effect of pipeline diameter and water depth on the scour hole discharge. The effect of the scour depth on the scour hole discharge was not considered; which will be taken into account in this study.

As discussed previously, the potential flow theory (equation (1)) often overestimates the scour hole discharge and scour depth due to its potential flow assumption. In this study, the turbulent model is employed to obtain more accurate flow field, thus to improve the prediction of the scour hole discharge as well as the scour depth.

2.1 Numerical Model

2.1.1 Governing Equations

The governing equations for the flow around the submarine pipeline are the continuity equation and the momentum equation:

$$\frac{\partial u_i}{\partial x_i} = 0 \quad (4)$$

$$\frac{\partial u_i}{\partial t} + u_j \frac{\partial u_i}{\partial x_j} = -\frac{1}{\rho} \frac{\partial p}{\partial x_i} + \frac{\partial}{\partial x_j} (2\nu S_{ij} - \overline{u_i u_j}) \quad (5)$$

where u_i is the flow velocity component in i direction; p is the pressure; ρ is the fluid density; ν is the fluid kinetic viscosity; u_i' is the fluctuation of flow velocity in i direction; S_{ij} is the mean strain rate tensor; $\overline{u_i u_j}$ is Reynold's stress tensor. S_{ij} and $\overline{u_i u_j}$ can be calculated by:

$$S_{ij} = \frac{1}{2} \left(\frac{\partial u_i}{\partial x_j} + \frac{\partial u_j}{\partial x_i} \right) \quad (6)$$

$$\overline{u_i u_j} = \nu_T \left(\frac{\partial u_i}{\partial x_j} + \frac{\partial u_j}{\partial x_i} \right) + \frac{2}{3} k \delta_{ij} \quad (7)$$

where ν_T is the turbulence viscosity; δ_{ij} is the Kronecker delta; k is the turbulent kinetic energy. The turbulent kinetic energy k and its dissipation rate ε can be simulated using the standard k - ε turbulence model:

k equation:

$$\frac{\partial(\rho k)}{\partial t} + \frac{\partial(\rho k u_i)}{\partial x_i} = \frac{\partial}{\partial x_j} \left[\left(\mu + \frac{\mu_t}{\sigma_k} \right) \frac{\partial k}{\partial x_j} \right] + G_k - \rho \varepsilon \quad (8)$$

ε equation:

$$\frac{\partial(\rho \varepsilon)}{\partial t} + \frac{\partial(\rho \varepsilon u_i)}{\partial x_i} = \frac{\partial}{\partial x_j} \left[\left(\mu + \frac{\mu_t}{\sigma_\varepsilon} \right) \frac{\partial \varepsilon}{\partial x_j} \right] + C_{1\varepsilon} \frac{\varepsilon}{k} G_k - C_{2\varepsilon} \rho \frac{\varepsilon^2}{k} \quad (9)$$

where μ is the fluid dynamic viscosity; μ_t is the turbulent eddy viscosity; G_k is the

generation of k induced by the mean velocity gradients. μ_t and G_k can be calculated by:

$$\mu_t = C_\mu \rho \frac{k^2}{\varepsilon} \quad (10)$$

$$G_k = 2\mu_t S_{ij} \frac{\partial u_i}{\partial x_j} \quad (11)$$

The constants in the k - ε model are taken from Rodi (1993): $C_\mu=0.09$, $C_{1\varepsilon}=1.44$, $C_{2\varepsilon}=1.92$, $\sigma_k=1.0$, and $\sigma_\varepsilon=1.03$.

2.1.2 Numerical schemes and validation case

Given the complex geometry considered, the computational domain is discretized using the unstructured meshes generated from mesh generation software ICEM in order to accurately fit the physical solid boundaries (Guo *et al.*, 2014). This allows for local refinement of the concerned regions (e.g. near the pipeline and sandy bed) with small meshes and has the advantage of flexibly assigning meshes in the computational domain (Jing *et al.* 2009; Guo *et al.*, 2012). In particular, near the seabed and pipe, a boundary layer mesh with a dimensionless nearest mesh size on the wall of between 30 and 500 is found to be optimum. The governing equations and turbulence equations are discretized by the finite volume method (FVM). The established SIMPLEC algorithm is used for pressure-velocity coupling. The momentum equation is solved by the QUICK scheme. The maximum residual number for convergence is taken as 10^{-5} and the time step is set as 0.005s.

The numerical model for flow simulation is validated using the laboratory experiments conducted by Jensen *et al.* (1990). The experiments were carried out in a 10 m (length) x 0.3 m (width) x 0.3 m (depth) flume. Water depth y_0 was kept as a constant of 0.23m. The diameter of the pipe tested was $D=0.03$ m. The velocity field was measured when the

equilibrium scour was reached. More details of the experiments can be found in Jensen et al. (1990).

The computational domain is shown in Figure 1 in which a Cartesian coordinate system is established. The bottom profile is the same as the equilibrium scour bed measured by Jensen *et al* (1990) in which the maximum scour depth $d_s/D=0.679$. The distance from the upstream boundary and the downstream boundary to the center of the pipeline is the same and is equal to $20D$.

At the inlet boundary, the vertical velocity profiles are specified using a power law function (Coles, 1956; Yang et al. 2012):

$$u(y) = u_m \left(\frac{y}{y_0} \right)^m \quad (12)$$

where u_m is the upstream flow velocity at $y=y_0$ (see Figure 1) and is specified using the experimental measurements; y is the vertical distance from the bed; m is the index number and is taken as $1/6$ (Yang *et al.*, 2012). Upstream flow velocity at the free water surface u_m is related to the average velocity by $u_m = u_0(m+1)$, where u_0 is the upstream average flow velocity (Yang *et al.*, 2012).

The outlet boundary is set as outflow boundary condition in which a static pressure at the outlet boundary is specified (Guo, 2014). The variation of water surface is small and can be ignored. The symmetric condition is set at the upper boundary. In this paper, the flow field around the submarine pipeline is simulated and the equilibrium scour profile is used to estimate the scour hole discharge at the equilibrium scour bed. As such, the sandy bed is set as a wall boundary condition where no slip condition is applied. The surface roughness height k_s is set as $2.5d_{50}$ and the standard wall function law is used to estimate the velocity parallel to the slope bed at the first cell (Launder and Spalding 1974).

After the numerical model is validated, the effect of the scour depth on the scour hole

discharge can be investigated by simulating the flow field around the submarine pipeline for a range of the fixed scour profiles described by (Dey and Singh 2008):

$$\frac{y_b}{d_s} = a_0 + a_1\left(\frac{x}{d_s}\right) + a_2\left(\frac{x}{d_s}\right)^2 + a_3\left(\frac{x}{d_s}\right)^3 \quad (13)$$

where a_0, a_1, a_2 and a_3 are parameters and taken as -0.931, -0.178, 0.124, and -0.01 respectively (Dey and Singh 2008). Differentiating Eq.(13) and setting it equal to zero yields the location $x/d_s=0.8$ where the maximum scour depth takes place. Equation (13) shows that at the section crossing the central axis of the pipeline, the scour depth d_c is $0.931 d_s$. This demonstrates that if d_c is known, the maximum scour depth can be estimated.

As the scour profiles for different maximum scour depths are known, the flow fields around the submarine pipeline over the scoured beds can be computed using the validated numerical model. The mesh strategy, solution methods and boundary conditions are kept the same as the validating case. The computational cases are: relative water depth $y_0/D=3, 5, 9$; upstream incoming average flow velocity $u_0=0.1, 0.2, 0.3, 0.4, 0.5$ m/s; the maximum scour depth $d_s/D=0.4\sim 1.7$; pipe diameter $D=0.03\text{m}$ and 0.1m . The sediment size $d_{50} =0.1, 0.3, 1.0$ and 3.0mm .

2.2 Prediction of scour depth

When the scour hole discharge is obtained from the numerical simulations, a fitted formula based on numerical results is proposed for convenience to calculate the scour hole discharge. The average flow velocity V in the scour hole at the section crossing the central axis of the pipeline (i.e. $x/D=0$) can be expressed as:

$$V = q_g / d_c \quad (14)$$

Using the average flow velocity V , the bed shear stress can be estimated as:

$$\tau_b = \lambda \frac{\rho}{8} V^2 \quad (15)$$

where λ is the friction coefficient, which can be obtained using the Colebrook-White equation (Dey and Singh, 2007):

$$\frac{1}{\sqrt{\lambda}} = -0.86 \ln \left(\frac{k_s}{3.7d_c} + \frac{2.51}{(\text{Re})_s \sqrt{\lambda}} \right) \quad (16)$$

where $(\text{Re})_s$ is the Reynolds number based on the scour depth, $(\text{Re})_s = \frac{Vd_c}{\nu}$, ν is fluid viscosity.

The dimensionless bed shear stress, the Shields number θ is employed (Shields 1936) to predict the incipient of the sediment movement:

$$\theta = \frac{\tau_b}{\rho g (s-1) d_{50}} \quad (17)$$

where s is the ratio of the sediment density over water density, d_{50} is the median sediment size of which 50% by weight is finer. The critical Shields number θ_{cr} for the incipient motion of sediment can be estimated as (Solusby and Whitehouse 1997):

$$\theta_{cr} = \frac{0.30}{1+1.2D_*} + 0.055 \left[1 - \exp(-0.020D_*) \right] \quad (18)$$

where D_* is the dimensionless sediment diameter, defined as:

$$D_* = \left[\frac{g(s-1)}{\nu^2} \right]^{1/3} d_{50} \quad (19)$$

Using these equations, the scour depth can be predicted using the following iterative procedure:

(1). Assuming a value of scour depth d_c and to calculate $d_s = 1.074d_c$.

(2). Using the fitted formula to calculate the scour hole discharge q_g . The average flow velocity V is then calculated using Eq.(14).

(3). Solving Eq.(16) by iteration to obtain λ . The bed shear stress τ_b is then computed using Eq.(15).

(4). Using Eq.(18) to calculate θ_{cr} , and then calculate the critical bed shear stress τ_{cr} using Eq.(17).

(5). Repeating steps 1 to 4 until

$$\frac{\tau_b - \tau_{cr}}{\tau_{cr}} < error \quad (20)$$

where *error* is the computational accuracy. The scour depth d_c is then the true value.

(6). The maximum scour depth d_s is now calculated as $d_s=1.074d_c$.

It should be noted that in Step (2), if the scour hole discharge is calculated using Eq.(1) or Eq.(3) instead of the fitted formula based on numerical results of this study, the scour depth obtained will be the results using the C-H method (Eq.(1)) or the Chiew method (Eq.(3)).

3 Results and discussions

3.1 Flow field

Figure 2 shows the typical streamlines around the pipeline for $u_0=0.2\text{m/s}$ over the equilibrium scoured bed at a certain time. It is seen that flow is split into two parts with one flowing through the scour hole and another flowing over the pipeline. A vortex is seen to be generated in the lee-wake region. To investigate the details of the flow structure within the scour hole and to verify the accuracy of the numerical simulation, Figure 3 compares the simulated (solid lines) and measured (open circles, Jensen et al. 1990) vertical velocity

profiles in the x direction at five different cross sections: $x/D=-3,-1, 0,1$ and 3 ; representing the upstream, right cross and downstream of the pipe. At the section of $x/D=-3$, the velocity profile is similar to that at the inlet, showing that the effect of the pipe and the scour hole on the far upstream flow velocity field is insignificant. The section of $x/D=-1$ is in front of the pipe where the flow velocity increases with the vertical distance from the bed. A relatively sharp increase of the flow velocity is seen to take place in the scour hole, i.e. $y \leq 0$ m. The flow velocity then increases slightly with the height for $0.00-0.03$ m, mainly due to the blocking effect of the pipe. This is followed by a gradual increase of the flow velocity with the distance from the sand bed. At the section crossing the central axis of the pipe, i.e. $x/D=0$, a sharp increase of the flow velocity with the vertical distance from the sand bed takes place both in the scour hole and above the pipe. The flow velocity then reaches the maximum value near the bottom of the pipe as well as immediately above the pipe. The flow velocity above the pipe is similar to that of the open channel flow while the velocity below the pipe (e.g. in the scour hole) decreases sharply and reaches zero at the scour hole bottom. The section of $x/D=1$ is in the lee-wake region where the existence of the negative flow velocity indicates that a pair of vortices are generated by water flowing around the pipe (see also Figure 2). No backflow is found at the section of $x/D=3$, indicating that the vortices disappear at that distance away from the pipe downstream. An S-shaped velocity profile is found in the lee side for $x/D=1$ and $x/D=3$. Figure 3 also shows that the simulated vertical flow velocity profiles agree reasonably well with the experimental measurements, demonstrating the accuracy of the numerical models for simulating such flows.

3.2 Effect of sediment size

To investigate the effect of sediment size on the scour hole discharge and the bed shear stress, simulations are performed for $d_{50} = 0.1\text{mm}, 0.3\text{mm}, 1\text{mm}$ and 3mm . The simulated flow velocity distribution in the scour hole for various sediments is used to obtain the scour hole discharge per unit width (q_g) by integrating the flow velocity over the scour depth. The results are plotted in Figure 4 in which the scour hole discharge per unit width q_g is normalized using the inflow discharge per unit width q_0 . It is seen that the sediment size has little effect on the relative scour hole discharge in the simulation range.

The bed shear stress is calculated from the numerical simulations with the standard wall function for $d_{50} = 0.1\text{mm}, 0.3\text{mm}, 1\text{mm}$ and 3mm ; two scour depth $d_s/D = 0.7$ and 1.0 and $u_0 = 0.2\text{m/s}$. The results are plotted in Figure 5. It is seen from Figure 5 that the bed shear stress increases significantly with the increase of the sediment size. This may be ascribed to the fact that the larger sediment particles generate a larger flow velocity gradient near the bed, leading to the sharp increase of the bed shear stress. Figure 5 also demonstrates that the scour hole depth has great impact on the bed shear stress. In general, the smaller scour hole depth generates a larger bed shear stress. This is because that the smaller scour hole depth has greater blocking impact to the flow, thus producing a greater velocity gradient near the scour hole bed and resulting in a greater bed shear stress.

3.3 Scour hole discharge

As analyzed above, the effect of the sediment size on the scour hole discharge is negligible. As such, it is possible to develop a formula from the numerical simulation to

calculate the scour hole discharge and compare with the results obtained by using the potential flow theory (the C-H method, equation (1)) and Chiew's method (equation (3)). To this end, fourteen maximum scour depths and two water depths are simulated. Figure 6 shows the comparison of the scour hole discharge obtained by present numerical model and by Eq.(1) and Eq.(3). It is seen that the scour hole discharge calculated from Eq. (1) is larger than that from present numerical model. This is because that the potential flow theory assumes an ideal fluid in which the viscosity of the fluid is not considered. Consequently, the potential flow theory will produce larger values of velocity and discharge in the scour hole. The scour hole discharge calculated by Eq. (3) does not change with the scour depth as the equation is only a function of the relative water depth and does not include the effect of the scour depth. The present numerical simulation results in Figure 6 also reveal that the water depth has little effect on the scour hole discharge. This may be ascribed to the fact that the flow above the pipe (beyond the scour hole) has negligible impact on the flow field (thus discharge) in the scour hole. Consequently, a best fit equation from the results generated by present numerical model can be obtained by ignoring the effect of water depth. Conducting the best fit for the simulated results yields:

$$\frac{q_g}{q_0} = -0.1681(d_s / D)^2 + 1.0556(d_s / D) + 0.0206 \quad 0.4 \leq d_s / D \leq 1.7 \quad (21)$$

3.4 Bed shear stress

When the scour hole discharge is calculated using Eq.(21), the bed shear stress can be estimated using the Colebrook-White equation as detailed in Section 2.2. As discussed before, the bed shear stress can also be directly calculated using the standard wall function in the

numerical model. Figure 7 shows the comparison of the bed shear stress obtained from the numerical simulation with the standard wall function and the Colebrook-White equation, respectively. It can be seen that for the case of the lower incoming flow velocity and smaller sediment particles, the bed shear stresses obtained by the two methods agree well with each other. When the sediment size and the flow velocity increase, the bed shear stress obtained from the numerical model is slightly larger than that obtained using the Colebrook-White equation. This study shows that, in general, the Colebrook-White equation can be used to calculate the bed shear stress with satisfactory accuracy.

3.5 Comparison with experiments

The results of 92 laboratory experimental data sets from Dey and Singh (2008) are used to evaluate the accuracy of the proposed method. The ranges of the experimental parameters are: $y_0/D = 3-7$; $u_0 = 0.242-0.645$ m/s; $D = 0.03-0.07$ m; $d_{50} = 0.48-3.0$ mm; $d_s/D = 0.7-1.66$. Present method as well as the C-H method and Chiew method is used to predict the scour depth. The predicted dimensionless scour depths using these three methods are compared with the measurements, as shown in Figures 8, 9 and 10, respectively. It is seen from Figure 8 that the C-H method significantly over-predicts the scour depth. All of the predicted scour depths are larger than the measured ones with most of the predicted scour depths being over 2.0 times the measurements. This is mainly due to the fact that Eq.(1) was derived from the potential flow theory and significantly overestimates the scour hole discharge and the bed shear stress. Figure 9 shows that the majority of the predicted scour depths using Chiew's method are larger than the measurements. On the other hand, Figure 10 shows that the

predicted scour depth using the present method is in good agreement with the measured values, indicating that the present method can be used to predict the scour depth around the submarine pipeline with satisfactory accuracy.

To compare the predicted scour depths using the three methods and the measurements in more detail, Table 1 lists the number of predicted cases falling in different error regions using the three methods for a wide range of sediment sizes. The absolute relative error in Table 1 is defined as $ARER = |(\text{predicted scour depth} - \text{measured scour depth})| / \text{measured scour depth}$. Table 1 reveals that there are only 4 cases (of 92 cases) whose ARER predicted using the present method is larger than 50%, while the numbers of cases using the C-H method and Chiew method are 89 and 12, respectively. In summary, the average absolute relative errors for all cases are 0.91, 0.24 and 0.18 by the C-H method, Chiew method and present method, respectively, showing that the present method is much more accurate than the other two methods.

3.6 Engineering Application

The present method is used to estimate the scour of Chengdao submarine pipeline in Shandong Province, China. The measured flow velocity is 0.65m/s, the water depth is 5m, the pipeline diameter is 0.5m and the sediment size is $d_{50}=0.05\text{mm}$. Using these field data and the present method, the maximum scour depth estimated is about 1.64m. The surveyed maximum scour depth is about 1.33m, which is slightly smaller than that predicted by present method. This discrepancy may be ascribed to the fact that the field conditions are different from the

laboratory conditions, which are the main common shortcomings of the physical model studies. For example, the relative water depth in the field is higher than that in laboratory conditions, and the incipient condition of sediment in the field is also higher than that in laboratory conditions; while the validation of the present method is based on laboratory conditions. These result in the discrepancy between the estimation and the field measurement. The prediction accuracy of the present method could be improved by including field data. Nevertheless, the slightly over prediction of the scour depth by this method is safe for submarine pipelines in terms of preventing its damage due to the fatigue failure caused by vortex induced vibration within the scour hole.

4 Conclusions

Numerical studies have been conducted to evaluate the scour hole discharge under steady flow condition. The scour hole discharge is determined by solving the RANS equations with a standard $k-\varepsilon$ turbulence closure. The effect of the model parameters, including the relative scour depth d_s/D , and the flow Re on the scour hole discharge are investigated numerically. A fitted formula which links the relative scour hole discharge q_g/q_0 and the relative scour depth d_s/D is obtained. Using this formula, an iterative method is proposed to predict the maximum scour depth. The predicted maximum scour depth using the present method is in good agreement with the laboratory measurements of Dey and Singh (2008) as well as being more accurate than those using the methods of Chao and Hennessey (1972) and Chiew (1991). This demonstrates that the proposed method can be applied to accurately predict clear-water scour depth below submarine pipelines under steady flow conditions. Regarding the application of

the present method to predict the scour depth in practical engineering, the present method may slightly overestimate the scour depth. This may be because that the critical bed shear stress used in the present method is based on laboratory conditions, which are different from those in real field. Further studies to include field measurements are required to improve the prediction accuracy.

Acknowledgements

This study was financially supported by the National Nature Science Fund of China (Grant No.50879084, 51279189), the Open Fund from the State Key Laboratory of Hydraulics and Mountain River Engineering, Sichuan University (SKHL1302), China Scholarship Council, Public Projects of Zhejiang Province (2016C33095) and the Natural Science Fund of Zhejiang Province (LQ16E090004). The constructive comments made by anonymous Reviewers have greatly improved the quality of the manuscript. The authors would like to thank Dr T. Sheehan for helping with the English writing.

References

- Brørs, B., 1999. Numerical Modeling of Flow and Scour at Pipelines. *Journal of Hydraulic Engineering*, 125(5), 511-523.
- Chao, J.L., Hennessy, P.V., 1972. Local scour under ocean outfall pipe-lines. *Journal of the Water Pollution Control Federation*, 44(7), 1443-1447.
- Chiew, Y.M., 1991. Prediction of maximum scour depth at submarine pipelines. *Journal of Hydraulic Engineering*, 117(4), 452-466.

- Coles, D.,1956.The law of wake in the turbulent boundary layer. *Journal of Fluid Mechanics*,1,191-226.
- Dey,S.,Singh,N.P.,2007.Clear-water scour depth below underwater pipelines. *Journal of Hydro-environment Research*, 1(2),157-162.
- Dey, S., Singh,N.P.,2008.Clear-water scour depth below underwater pipelines under steady flow. *Journal of Hydraulic Engineering*, 134(5), 588-600.
- Guo,Y.K., Wu,X.G., Pan,C.H., Zhang,J.S., 2012. Numerical simulation of the tidal flow and suspended sediment transport in the Qiantang Estuary. *Journal of Waterway, Port, Coastal and Ocean Engineering*, 138(3), 192-203.
- Guo, Y.K. (2014). “Numerical simulation of the spreading of aerated and nonaerated turbulent water jet in a tank with finite water depth.” *Journal of Hydraulic Engineering*, 140(8). DOI: [10.1061/\(ASCE\)HY.1943-7900.0000903](https://doi.org/10.1061/(ASCE)HY.1943-7900.0000903).
- Guo, Y.K., Zhang, Z.Y., and Shi, B. (2014). “Numerical simulation of gravity current descending a slope into a linearly stratified environment.” *Journal of Hydraulic Engineering*, 140 (12), DOI: [10.1061/\(ASCE\)HY.1943-7900.0000936](https://doi.org/10.1061/(ASCE)HY.1943-7900.0000936).
- Ibrahim, A., Nalluri, C.,1986. Scour prediction around marine pipelines. *Proceedings of the 5th International Symposium on Offshore Mechanics and Arctic Engineering*, Tokyo, Japan. pp.679-684.
- Jensen, B.L., Sumer, B.M., Jensen, H.R., Fredsøe, J.,1990. Flow around and forces on a pipeline near a scoured bed in steady current. *Journal of offshore Mechanics and Arctic Engineering*, 112(1),206-213.

- Jing, H., Guo, Y.K., Li, C. and Zhang, J. (2009). "Three dimensional numerical simulation of compound meandering open channel flow by Reynolds stress equation model." *International Journal for Numerical Methods in Fluids*, 59:927-943.
- Kamphuis, J.W., 1974. Determination of Sand Roughness for Fixed Beds. *Journal of Hydraulic Research*, 12(2), 193-202.
- Kjeldsen, S.P., Gjorvik, C., Bringaker, K.G., Jacobsen, J., 1973. Local scour near offshore pipelines. *Proceedings the second International Conference on Port and Ocean Engineering Under Arctic Conditions*, Reykjaik, Iceland. pp309-331.
- Lauder, B.E., and Spalding, D.B. (1974). "The numerical computation of turbulent flows." *Computer Methods in Applied Mechanics and Engineering*, 3, 269–289.
- Liang, D.F., Cheng, L., Li, F., 2004. Numerical modelling of scour below a pipeline in currents. part II: Scour simulation. *Coastal Engineering*, 52(1), 43-62.
- Liang, D.F., Cheng, L., Yeow, K., 2005. Numerical study of the Reynolds-number dependence of two-dimensional scour beneath offshore pipeline in steady currents. *Ocean Engineering*, 32(13), 1590-1607.
- Moncada-M, A.T., Aguirre-Pe, J., 1999. Scour below pipeline in river crossings. *Journal of Hydraulic Engineering*, 125(9): 953-958.
- Rodi, W., 1993. Turbulence models and their application in hydraulics: a state-of-the-art review. 3rd edition, A.A. Balkema, Rotterdam, Netherlands.
- Shields, A., 1936. Application of similarity principles and turbulence research to bed-load movement. *Mitteilungen der Preussischen Versuchsanstalt für Wasserbau und Schiffbau* 26, 5-24.

Soulsby, R., Whitehouse, R., 1997. Threshold of sediment motion in coastal environments.

Proc. Pacific Coasts and Ports 1997 Conf., Christchurch, New Zealand, 1, 149-154.

Yang, L.P., Shi, B., Guo, Y.K., Wen, X.Y., 2012. Calculation and experiment on scour depth for submarine pipeline with a spoiler. *Ocean Engineering*, 55, 191-198

Yasa, R., 2011. Prediction of the Scour Depth under Submarine Pipelines-in Wave Condition. *Journal of Coastal Research*, SI64, 627-630.

Yeganeh-Bakhtiary, A., Kazeminezhad, M.H., Etemad-Shahidi, A., Baas, J.H., Cheng L., 2011. Euler-Euler two-phase flow simulation of tunnel erosion beneath marine pipelines. *Applied Ocean Research*, 33, 137-146.

Zhao, Z.H., Fernando, H.J.S., 2007. Numerical simulation of scour around pipelines using an Euler-Euler coupled two-phase model. *Environment Fluid Mechanics*, 7, 121-142.

Zhao, M., Cheng, L., 2008. Numerical modeling of local scour below a piggyback pipeline in currents. *Journal of Hydraulic Engineering*, 134(10), 1452-1463.

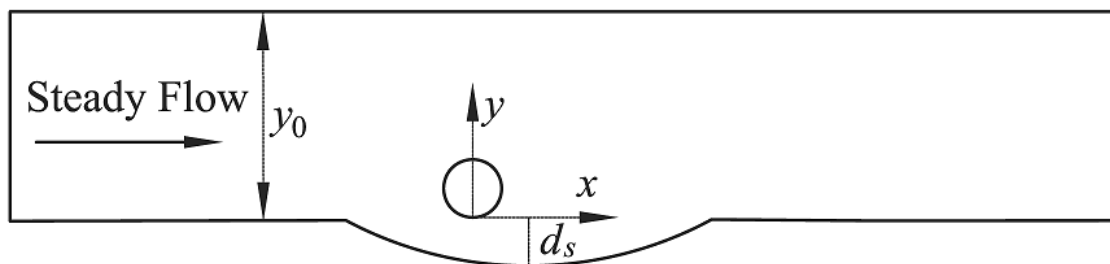


Figure 1. Sketch of the computational domain

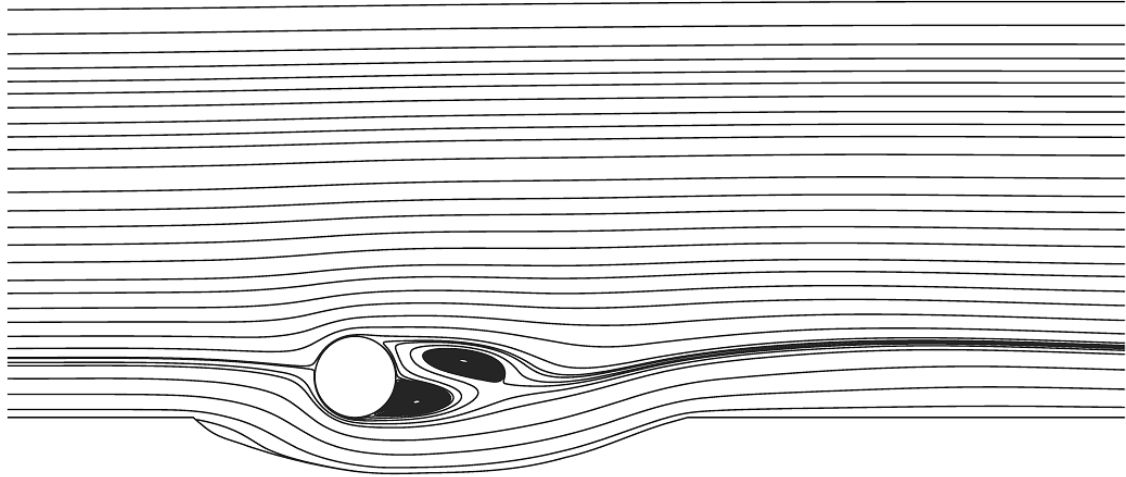


Figure 2. Simulated flow streamlines for validating case: $u_0=0.2\text{m/s}$

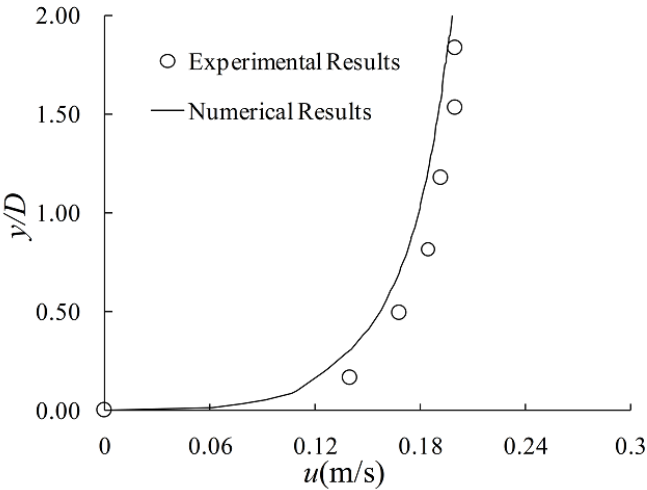


Figure 3(a)

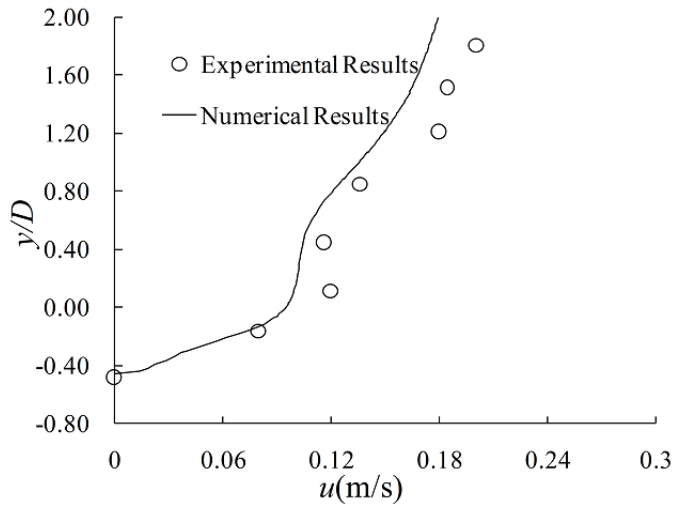


Figure 3(b)

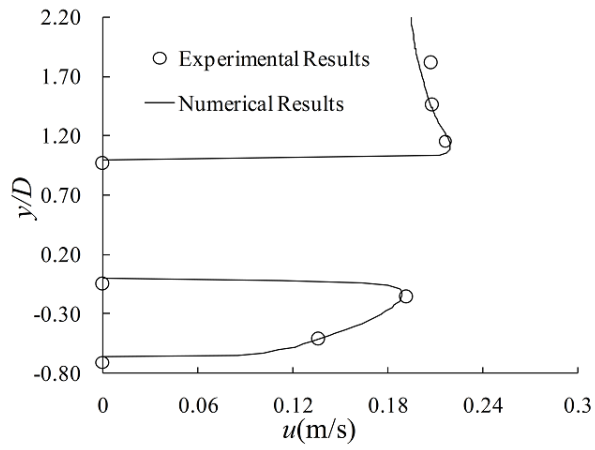


Figure 3(c)

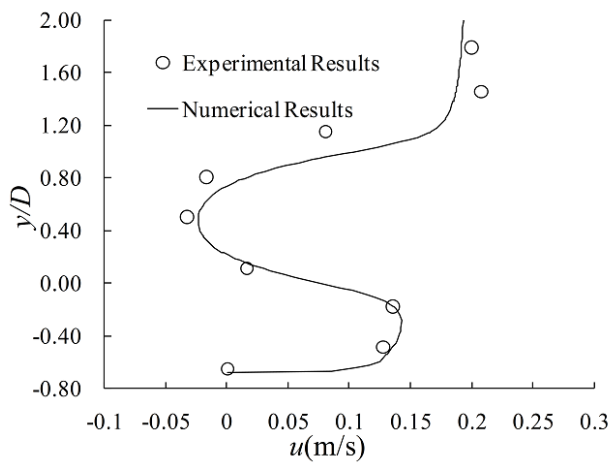


Figure 3(d)

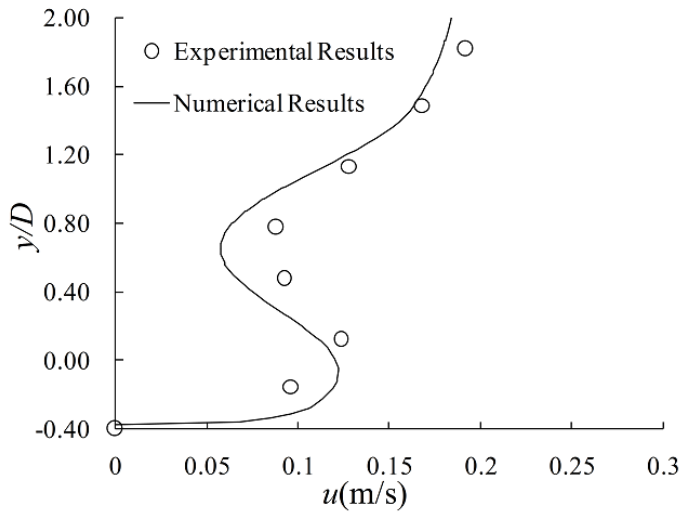


Figure 3(e)

Figure 3. Comparison of the simulated (solid lines) and measured (open circles, Jensen et al.

1990) vertical velocity profiles at five cross sections along flow direction for $u_0=0.2\text{m/s}$:

(a) $x/D=-3$; (b) $x/D=-1$; (c) $x/D=0$; (d) $x/D=1$; (e) $x/D=3$; representing the upstream,

right cross and downstream of the pipe

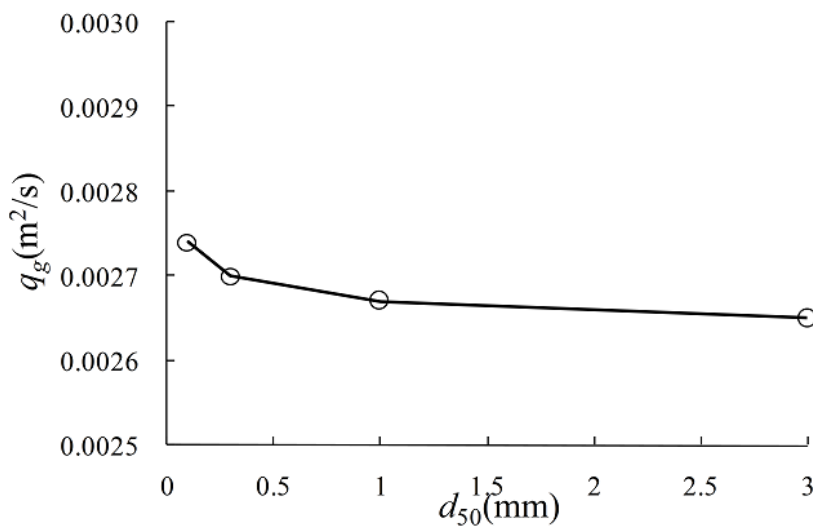


Figure 4. Variation of the simulated relative scour hole discharge qg/q_0 with the sediment size

d_{50} for $u_0=0.2\text{m/s}$ and $d_s/D=0.7$

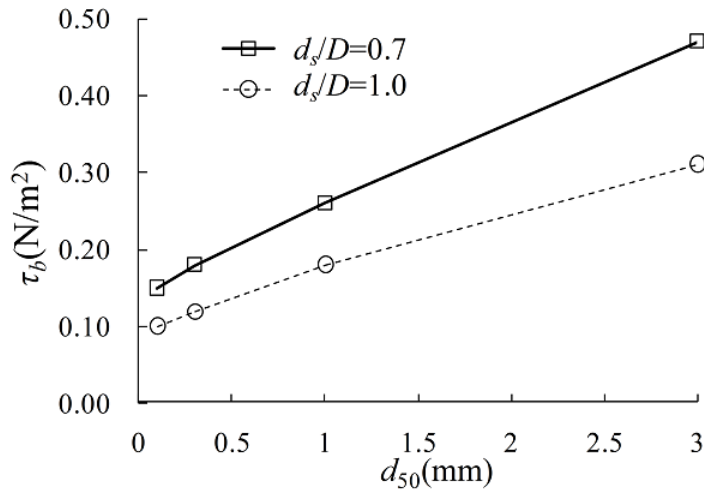


Figure 5. Variation of the simulated bed shear stress τ_b with the sediment size d_{50} for $u_0=0.2\text{m/s}$ and two scour depths indicated

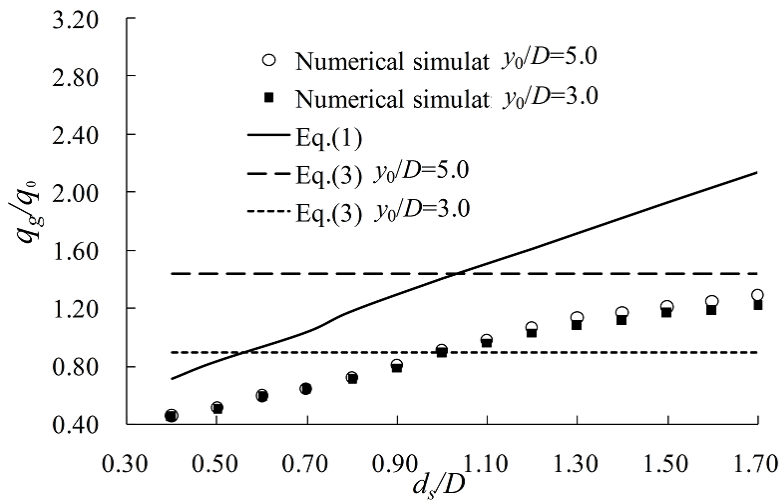


Figure 6. Comparison of the relative scour hole discharge using Eq(1), Eq(2) and Eq(20)

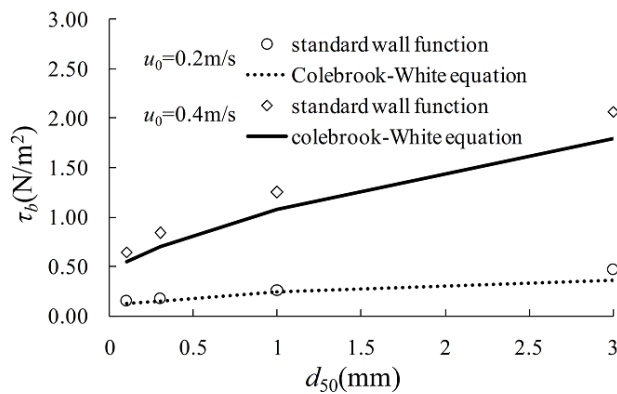


Figure 7. Comparison of the bed shear stress predicted by the present method and the

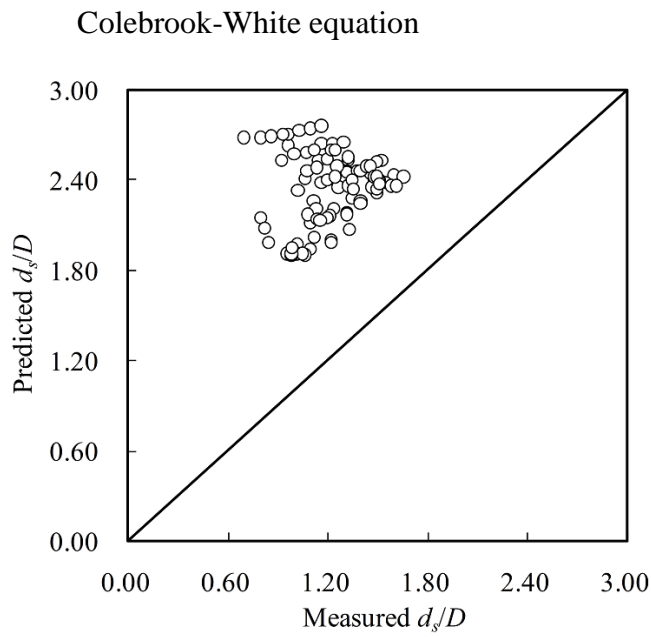


Figure 8. Comparison between the predicted scour depth using the C-H method and the measurements

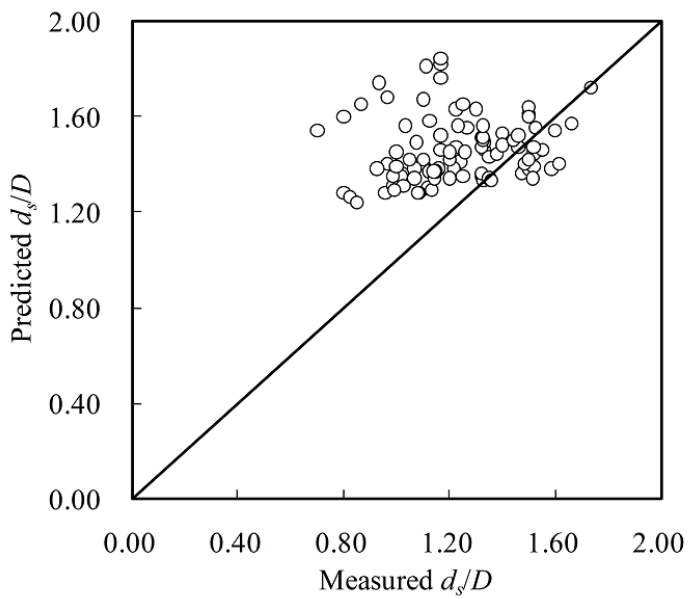


Figure 9. Comparison between the predicted scour depth using the Chiew method and the measurements

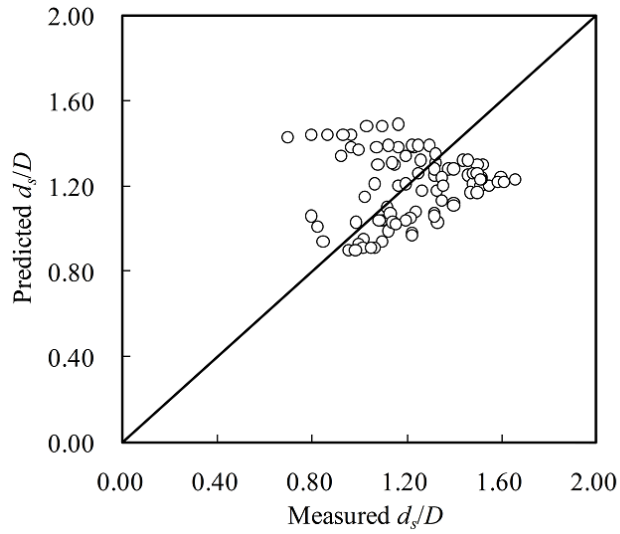


Figure 10. Comparison between the predicted scour depth using the present method and measurements

Table 1. The distributions of absolute relative error of predicted scour depth using different methods.

d_{50} (mm)	Methods	No. $ARER \leq 0.2$	No. $0.2 < ARER \leq 0.5$	No. $0.5 < ARER \leq 1.0$	No. $1.0 < ARER$	Average ARER
0.45	C-H	-	-	15	3	0.92
	Chiew	4	12	2	-	0.31
	Present	13	5	-	-	0.14
0.81	C-H	-	-	15	4	0.82
	Chiew	15	4	-	-	0.15
	Present	15	4	-	-	0.13
1.86	C-H	-	-	13	6	0.83
	Chiew	15	4	-	-	0.11
	Present	12	7	-	-	0.16
2.54	C-H	1	-	8	7	1.24
	Chiew	9	2	3	2	0.37
	Present	10	2	3	1	0.30
3.00	C-H	-	2	7	11	1.04
	Chiew	9	6	5	-	0.27
	Present	10	10	-	-	0.20
Total	C-H	1	2	58	31	0.91
	Chiew	52	28	10	2	0.24
	Present	60	28	3	1	0.18